

# An Analytical Study of Peer-to-Peer Media Streaming Systems

Yi-Cheng Tu

Department of Computer Sciences, Purdue University

Jianzhong Sun

Department of Mathematics, University of North Carolina Wilmington

Mohamed Hefeeda

School of Computing Science, Simon Fraser University Surrey, Canada

Sunil Prabhakar

Department of Computer Sciences, Purdue University

---

Recent research efforts have demonstrated the great potential of building cost-effective media streaming systems on top of peer-to-peer (P2P) networks. A P2P media streaming architecture can reach a large streaming capacity that is difficult to achieve in conventional server-based streaming services. Hybrid streaming systems that combine the use of dedicated streaming servers and P2P networks were proposed to build on the advantages of both paradigms. However, the dynamics of such systems and the impact of various factors on system behavior are not totally clear. In this paper, we present an analytical framework to quantitatively study the features of a hybrid media streaming model. Based on this framework, we derive an equation to describe the capacity growth of a single-file streaming system. We then extend the analysis to multi-file scenarios. We also show how the system achieves optimal allocation of server bandwidth among different media objects. The unpredictable departure/failure of peers is a critical factor that affects the performance of P2P systems. We utilize the concept of *peer lifespan* to model peer failures. The original capacity growth equation is enhanced with coefficients generated from peer lifespans that follow an exponential distribution. We also propose a failure model under arbitrarily distributed peer lifespan. Results from large-scale simulations support our analysis.

Categories and Subject Descriptors: H.1 [Information Systems]: Models and Principles

General Terms: performance

Additional Key Words and Phrases: media streaming, peer-to-peer, media-on-demand

---

## 1. INTRODUCTION

Multimedia streaming over the Internet has become a reality with the development of media compression methods, high-throughput storage systems, and broadband networking technology. Attractive applications such as entertainment video-on-demand, digital libraries, and on-line news services built on top of real-time media streaming architectures are now publicly available. However, there are still many

---

This work is supported by NSF fund IIS-9985019.

Permission to make digital/hard copy of all or part of this material without fee for personal or classroom use provided that the copies are not made or distributed for profit or commercial advantage, the ACM copyright/server notice, the title of the publication, and its date appear, and notice is given that copying is by permission of the ACM, Inc. To copy otherwise, to republish, to post on servers, or to redistribute to lists requires prior specific permission and/or a fee.

© 2005 ACM 1529-3785/2005/0700-0001 \$5.00

challenges towards building cost-effective, robust and scalable multimedia streaming systems [Wu et al. 2001] due to the stringent bandwidth, packet loss and delay requirements for media streaming.

A majority of media streaming architectures follow a server/client design. In a large streaming system where user requests arrive at a high rate, a server has to support a large number of concurrent streaming sessions. Multiple servers or proxies can be deployed to increase total system capacity. In this design, media content is replicated on these proxies and clients receive streaming data from the closest proxy. There are two advantages of using proxies: (i) user requests are handled by all proxies with a combined capacity greater than the capacity provided by the single-server architecture; (ii) better QoS (in terms of latency and packet loss) in streaming due to the shortened packet delivery path. Such systems are sometimes called Content Distribution Networks (CDNs) [Biliris et al. 2002].

The cost of maintaining a CDN is extremely high considering the massive CPU power, storage space and bandwidth needed. As the service becomes more popular, more servers have to be deployed. One approach to solve the above problem is motivated by the emerging concept of peer-to-peer (P2P) computing [Milojicic et al. 2002; Rowstron and Druschel 2001a; Crowcroft and Pratt 2002]. In a P2P system, there is no centralized entity controlling the behavior of peers. Instead, each peer contributes its share of resources and cooperates with other peers according to some predefined rules for communications. In the context of media streaming, a well-organized community of clients can significantly lower the service load of CDN servers by taking over some of the streaming tasks. The basic idea is to let clients that have acquired a media object act as streaming servers for subsequent requests to that object. One of the key features of a P2P streaming system is that its total capacity grows when the content it manages becomes more popular [Xu et al. 2002]. This is the most important difference between P2P and the server/client paradigms.

Hybrid media streaming systems that combine centralized servers and peer-to-peer networks have been proposed in [Xu et al. 2003] and [Hefeeda et al. 2003]. As compared to a P2P-only architecture, the hybrid streaming system can disseminate media content faster and responds quicker to requests. System performance in media streaming services is mainly bottlenecked by bandwidth [Padmanabhan et al. 2002]. Some operations such as directory management and searching that consume less bandwidth can be processed at a centralized server for efficiency reasons. Furthermore, peers are heterogeneous in the duration of their commitment to the community [Saroiu et al. 2003]: each peer could leave or fail at any time. In order to minimize the effects of this come-and-go behavior, servers can act as backup resource providers even when the P2P network has enough capacity. Servers are qualified to play this role because of their robustness.

The focus of this paper is to study the features of a hybrid media streaming architecture by mathematical analysis. We are primarily interested in the pattern of system capacity growth and the effects of various factors on that growth. The system capacity is defined as the total streaming bandwidth available from both servers as well as peers. Conclusions drawn from such analysis improve our understanding of system dynamics and provide guidelines for the design and realization of media delivery services based on hybrid architectures. In this paper, we propose

a generic media streaming model that utilizes both a CDN and P2P network. The model differs from those found in [Xu et al. 2003] and [Hefeeda et al. 2003] in that it is applicable to a more general environment and is more amenable to quantitative analysis of system performance. Using a deterministic discrete-time analysis approach, we derive the growth equation for system capacity. This equation is used to analyze the time threshold at which the system capacity is sufficient to handle the total load. We extend the results from a single-file system to a multi-file system. We also show that our streaming architecture achieves near-optimal performance in terms of the time needed for a complete load hand-over from servers to peers. Furthermore, peer failures are factored into the analytical model. We study peer failures by associating a ‘lifespan’ with each peer and analyzing the system performance under different lifespan distributions. We also present two enhancements of the analysis. In the first, we analyze a media streaming system in which a peer can start serving a file to others before completely receiving it. We show that this overlapping of receiving and serving can significantly accelerate the capacity growth and reduce the server-peer transition time. In the second enhancement, we study a general multi-file streaming system in which files may have different lengths and bit rates. We describe how the optimal transition time can be computed numerically. In addition, we evaluate several performance metrics by extensive simulations, the results of which confirm the validity of our analysis.

This paper continues with Section 2 by comparing our research with related work. Then we introduce the streaming model in Section 3. We start our analysis by studying single-file systems without failures in Section 4. Then we extend to multi-file systems (Section 5) and systems with peer failures (Section 6). Two extensions of the main results are presented in Section 7. Section 8 presents the simulation results. We conclude the paper with Section 9.

## 2. RELATED WORK

A review on Internet video streaming can be found in [Wu et al. 2001]. The key research areas of video streaming are identified and methodologies are discussed. Research on P2P computing was greatly motivated by the success of Gnutella<sup>1</sup> and Napster<sup>2</sup>. The general philosophy and current research efforts of P2P computing are introduced in [Milojicic et al. 2002] and [Crowcroft and Pratt 2002]. Pastry [Rowstron and Druschel 2001a], Chord [Stoica et al. 2001], and CAN [Ratnasamy et al. 2001] are the most popular P2P searching/routing protocols. P2P applications built on top of these protocols are presented in [Rowstron and Druschel 2001b] and [Dabek et al. 2001]. Other topics of P2P research include system design [Ripeanu et al. 2002], traffic measurement [Saroiu et al. 2003], and usage of coupons/incentives [Horne et al. 2001; Golle et al. 2001].

In the context of peer-to-peer media streaming, both the CoopNet project [Padmanabhan et al. 2002] and the ZIGZAG prototype [Tran et al. 2003] explore how media streams should be delivered to many clients under the situation of flash crowd. Both projects concentrate on how to efficiently maintain a multicast tree in an environment where user behavior is unpredictable. CoopNet utilizes the method

<sup>1</sup><http://www.gnutella.com>

<sup>2</sup><http://www.napster.com>

of *Multiple Description Coding* (MDC) to deal with the in-session departure/failure of streaming peers. Our system model differs from these efforts in the sense that we focus on the delivery of on-demand media instead of live media. Commercial content delivery services such as Allcast<sup>3</sup> and C-Star<sup>4</sup> are close in spirit to on-demand P2P media streaming. In [Xu et al. 2002], an algorithm that assigns media segments to different supplying peers and an admission protocol for requests are introduced. [Nguyen and Zakhor 2002] emphasizes streaming protocol design. In their work, an RTP-like protocol with the features of rate control and packet synchronization is developed.

Research on hybrid media streaming architecture shown in [Xu et al. 2003] is directly related to our work. A similar P2P streaming architecture can be found in [Hefeeda et al. 2003] and [Hefeeda et al. 2004], in which efficient algorithms for dissemination of media content and economical analysis of P2P streaming services are presented. They show that, with small initial investment and the use of incentives, a large-scale and profitable media streaming service can be built.

Several recent efforts emphasize performance analysis of P2P networks. In [Yang and de Veciana 2004], a branching model and a Markov chain model are used to study the system dynamics of a BitTorrent<sup>5</sup>-like file sharing network in its transient and steady states, respectively. They find that the capacity of such systems grows exponentially in transient and stabilizes at steady state. The above work is extended in [Qiu and Srikant 2004] where a fluid model is exploited to quantify system capacity at steady state so that explicit expressions of performance metric are obtained (vs. numerical results obtained in [Yang and de Veciana 2004]). Furthermore, other features of the BitTorrent network such as downloading efficiency and incentives are discussed. In [Ramachandran and Sikdar 2005], downloading speed in similar systems are analyzed with consideration of network topology and peer heterogeneity. Our work differs from the above efforts in the following aspects:

1. We deal with P2P media streaming rather than file downloading. We study system capacity and transition time using a discrete-time analytical method;
2. We accomplish a quantitative analysis of the performance of a multi-file system and prove optimality in terms of the transition time of the system model. Ours is the only work that accomplishes this, to the best of our knowledge;
3. We explore the impact of peer failure under different failure models. Among them, the matrix model is not found in any other P2P research.

Among the above contributions, items 1 and 3 can be readily used to study pure-P2P streaming systems (i.e., those without servers). Our study greatly improves the analytical research on a hybrid streaming system presented in [Xu et al. 2003] as the latter only considers single-file system without failures. Finally, we extend the conference version of this paper [Tu et al. 2004] by relaxing several assumptions such that the analysis applies to more general cases of system operation. For instance, we study system performance under the effects of arbitrary distributions of peer lifespan (Section 6.2), shortened inter-session delays (Section 7.1), and variable

<sup>3</sup><http://www.allcast.com>

<sup>4</sup><http://www.centerspan.com>

<sup>5</sup><http://www.bittorrent.com>

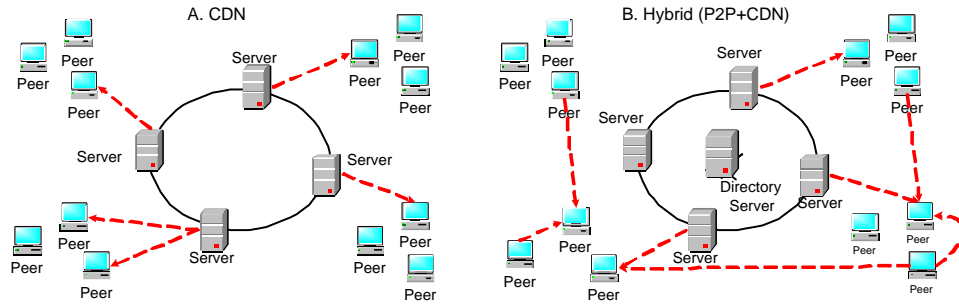


Fig. 1. A comparison between CDN and hybrid media streaming architectures. Dotted lines show the directions of the streaming.

streaming length and bitrate of media objects (Section 7.2). Due to the space limitation, some details of this study are not included in this paper and can be found in our technical report [Tu et al. 2005].

### 3. SYSTEM MODEL, ASSUMPTIONS, AND NOTATIONS

Our analysis is based on the media streaming infrastructure shown in Figure 1B. The model is similar to the hybrid structure proposed in [Xu et al. 2003] and [Hefeeda et al. 2003] with some modifications. The main entities of the system are:

- **Directory Server.** The role of the directory server is to maintain an index of media location (i.e. what peers hold copies of the media). It is also responsible for processing queries<sup>6</sup>.
- **Server.**<sup>7</sup> A server holds a copy of all media files and is responsible for streaming when the requested media cannot be served through the P2P network. Each server has a fixed bandwidth. We assume a zero downtime for the servers.
- **Peer (client).** The set of user machines participating in the streaming system are known as peers. A peer asking for a media object is called a *requesting peer* and a peer that has acquired any media object(s) is called a *qualified peer*. Upon joining the system, each peer announces its maximum bandwidth and storage contribution. We divide peers into a number of classes based on their bandwidth contributions. The average bandwidth contribution of peers in all classes is  $\alpha$ .
- **Media content.** The target resource a client requests. We can view this as a collection of media files. To simplify the analysis, we assume that all streams are Constant Bit Rate (CBR) media streams.

Figure 1B shows all entities in the hybrid streaming architecture and how they interact. For the sake of comparison, Figure 1A shows a CDN-based streaming architecture. Note that the main difference between the CDN architecture and the hybrid architecture is that client machines can be data senders in the latter.

<sup>6</sup>If we replace the directory server with non-centralized object lookup solutions (e.g. Pastry), our analysis still works as we focus on system throughput rather than lookup latency.

<sup>7</sup>In this paper, the terms ‘streaming server’, ‘CDN server’ and ‘server’ are used interchangeably.

In our model, the system operates as follows. When a peer requests a media object, it first sends out a query to the directory server. The directory server searches its local database and returns a list of available qualified peers and CDN servers to the requesting peer. We first choose CDN servers with available bandwidth as data senders. If all CDN servers are busy, the requesting peer chooses from the list of qualified peers a subset that satisfies the bandwidth and QoS requirements and the streaming starts.<sup>8</sup> The peers that act as data senders are called *supplying peers*. When the streaming is finished, the requesting peer becomes a qualified peer. If there is not enough bandwidth from both the servers and qualified peers, the request is rejected immediately (without waiting).

We model the arrival of streaming requests as a Poisson process with a time-invariant rate  $\lambda$ . We are interested in a system where the streaming capacity of the servers is small compared to the total capacity needed to handle all requests. In other words, servers act as ‘seeds’ for the media content and we expect that the streaming load will eventually be shifted to peers.

### 3.1 Assumptions

The system analysis is performed in a top-down manner. We start from a simple model with assumptions on the factors we are interested in and then enhance the results derived from the simple model by relaxing these assumptions. In the initial analysis, we make the following assumptions:

1. The system contains only one media file. In Section 5, the analysis is extended to multi-file systems;
2. Peers never fail. Peer failure is addressed in Section 6;
3. Requests are uniformly distributed among the peer population;
4. The bottleneck link for a streaming session can only be the upload link capacity of the data sender (CDN server or supplying peer); and
5. Each participating peer has infinite storage contribution. We shall see in Section 8 that only a small storage contribution is actually needed from each peer, which makes this a harmless assumption.

### 3.2 Metrics and Notations for Analysis

The total number of qualified peers and their bandwidth contributions are direct measures of system capacity. Our analysis focuses on these two metrics. Previous work [Xu et al. 2003] on hybrid streaming systems has shown that the streaming load can be fully taken over by peers after some time. This can be illustrated by

---

<sup>8</sup>The mechanism of selecting the subset of peers to stream the media object is orthogonal to the analysis presented in this paper. We note that there are a number of ways to perform the selection. A simple mechanism is to choose suppliers that are topologically close to the receiver based on IP addresses. This can be done by clustering peers in the system using their IP addresses [Hefeeda et al. 2004]. As another mechanism, the receiver could leverage Internet measurement infrastructures such as IDMaps [Francis et al. 2001] to measure relative distances between each potential supplier and itself. A third selection mechanism infers characteristics of the network paths connecting the potential suppliers. These characteristics are then used to select the best subset of suppliers [Hefeeda et al. 2003].

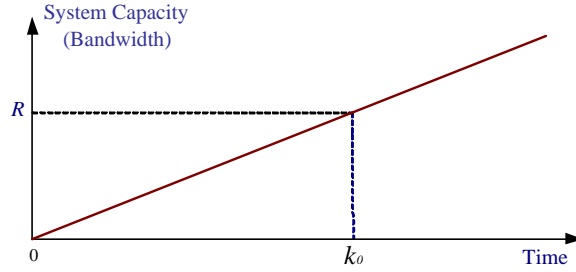


Fig. 2. Proposed peer bandwidth growth and transition point in the hybrid streaming architecture.

Figure 2 where the tentative system bandwidth is plotted. As more and more peers become qualified peers, we have reason to believe that the system capacity grows over time (not necessarily linear growth as shown in Figure 2). Suppose the total capacity required to handle all requests is  $R$ , then at a certain point in time, the system capacity outgrows  $R$ . This time point is called *server-peer transition time* (denoted as  $k_0$ ). Knowing  $k_0$ , we can modify the protocol to let the requesting peers obtain bandwidth from qualified peers first and use servers as backup sources of bandwidth after transition. For service providers,  $k_0$  can be used, for example, to indicate when server resources can be reallocated to stream other media objects, or to determine the length of their contracts with resource vendors.

Another metric we consider is *reject rate*. The reject rate at time  $x$  is defined as the ratio of total number of rejected requests to the total number of requests within a time interval  $[x - \Delta x, x + \Delta x]$ . Here we see that reject rate depends on the window size  $2\Delta x$ . Intuitively, reject rate decreases as system capacity increases.

Symbols used in the analysis are listed in Table I.

Table I. Notations and Symbols.

Symbol	Definition
$L$	Length of one streaming session
$k$	Discrete time index, each unit has a length of $L$
$N$	Total server bandwidth
$M$	Total number of peers
$\lambda$	Request rate to the system, in requests per unit time
$k_0$	Server-Peer transition time, in number of streaming periods
$P(k)$	Number of qualified peers at interval $k$
$C(k)$	Total system capacity (i.e. bandwidth) at interval $k$
$F$	Total number of media files
$b$	Bandwidth required to stream a file
$\alpha$	Average bandwidth contribution of all peers

#### 4. MAIN RESULT: SINGLE-FILE SYSTEM WITHOUT FAILURE

In this section, we focus our analysis on a system containing only one media file without considering peer failures. A salient feature of the media streaming application is that all streaming sessions of the same media object last for  $L$  time

units. This feature can be leveraged to analyze (qualified) peer population in a discrete-time manner. Suppose, within the  $k$ -th time interval (Figure 3), the system initiates  $n$  streaming sessions  $S_1, S_2, \dots, S_n$ . Then we are certain that the  $n$  requesting peers in these sessions will become qualified peers in the  $(k+1)$ -th interval as all sessions will terminate by the end of the next interval. To project the total number of qualified peers from period  $k$  to period  $k+1$ , we need to know how many sessions are initiated during period  $k$ .

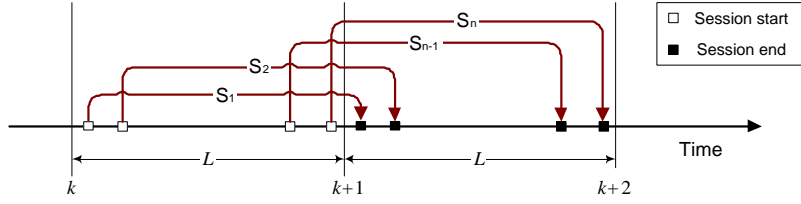


Fig. 3. Streaming sessions within a time interval of length  $L$ .

Before the server-peer transition time  $k_0$ , the bandwidth of both servers and qualified peers is fully utilized as demands are overwhelming. Therefore, the number of new qualified peers produced between two consecutive time intervals  $k$  and  $k+1$  can be expressed as:

$$P(k+1) - P(k) = \frac{N}{b} + P(k) \frac{\alpha}{b}, \quad 0 \leq k \leq k_0. \quad (1)$$

The two terms on the right-hand side of the above equation are the number of new qualified peers generated by servers and that of the qualified peers generated by previously qualified peers, respectively. Eq.(1) can be rewritten as

$$P(k+1) + \frac{N}{\alpha} = \left( P(k) + \frac{N}{\alpha} \right) \left( 1 + \frac{\alpha}{b} \right).$$

Solving the above geometric progression with  $P(0) = 0$ , we get

$$P(k) = \frac{N}{\alpha} \left[ \left( 1 + \frac{\alpha}{b} \right)^k - 1 \right]. \quad (2)$$

We name the term  $\frac{\alpha}{b}$  as the *capacity growth factor* of the system. The total system capacity (in terms of bandwidth) at interval  $k$  is thus given by:

$$C(k) = N + \alpha P(k) = N \left( 1 + \frac{\alpha}{b} \right)^k, \quad \text{for } k \leq k_0. \quad (3)$$

From the discussions in Section 3, we know that the total system capacity at  $k_0$  is equal to the capacity required to serve all requests. The total capacity needed to satisfy all requests in  $L$  time units is  $\lambda L b$ . Therefore, we have the following equation to solve  $k_0$ :

$$N \left( 1 + \frac{\alpha}{b} \right)^{k_0} = \lambda L b. \quad (4)$$

In the above equation,  $N, \alpha, \lambda, L, b$  are known constants, therefore we get  $k_0$  as

$$k_0 = \log_{(1+\frac{\alpha}{b})} \left( \frac{\lambda L b}{N} \right) = \frac{\lg(\lambda L b) - \lg N}{\lg(1 + \frac{\alpha}{b})}. \quad (5)$$

From Eq.(2), we also see that  $P(k_0) = \frac{N}{\alpha}(\frac{\lambda L b}{N} - 1)$  peers are needed in addition to the servers so that total system bandwidth is able to handle all subsequent requests. Note that the unit for  $k_0$  is time intervals rather than natural time units.

The above analysis (refer to Eq.(3)) shows an exponential growth pattern of system capacity, which is similar to the results of a recent study on P2P file sharing applications [Yang and de Veciana 2004]. The discrete-time analysis approach is also used in [Xu et al. 2003] and similar results (with numerical solution for  $k_0$ ) are found. We improve their analysis by giving a closed-form expression for the server-peer transition time.

*Remark 4.1.* In practice, the capacity growth factor  $\frac{\alpha}{b}$  is small (typically less than 1.0), because the average bandwidth contribution from a peer ( $\alpha$ ) is less than the bandwidth required to stream the media object ( $b$ ). As a result,  $k_0$  is almost linearly related to  $\frac{\alpha}{b}$  since

$$k_0 = \frac{\lg(\lambda L b) - \lg N}{\lg(1 + \frac{\alpha}{b})} \approx \frac{\lg(\lambda L b) - \lg N}{\frac{\alpha}{b}}.$$

This shows that  $k_0$  is more sensitive to  $\frac{\alpha}{b}$  than to  $\lambda$  and  $N$ . The effect of  $L$  on  $k_0$  is also similar to that of  $\lambda$  and  $b$ . Note that there is a super-linear relationship between  $L$  and the *absolute* transition time (denoted as  $T_0$ ).  $T_0$  is measured in natural time units rather than generations and is given by  $T_0 = Lk_0$ . In Section 7.2, we shall see more discussions on  $T_0$ .

*4.0.1 Dynamics of reject rate.* As mentioned earlier, there is no unique way to quantify the reject rate as it depends on the size of time window ( $\Delta x$ ) we use. Let us first discuss the scenario when window size is much smaller than  $L$ . An observation under such circumstances is: in early streaming periods, the majority (if not all) of streaming sessions start at the very beginning of that period. This is due to the heavy load put to the system: bandwidth is quickly utilized and all subsequent requests in that period will be rejected. As a result, the reject rate is close to zero at the beginning and reaches almost 100% until the end of the current streaming period. The above pattern repeats itself in every streaming period. However, within each cycle, the time when the reject rate is low becomes longer as system capacity grows. At period  $k_0$ , the reject rate for the whole streaming period will be low. In other words,  $k_0$  can be viewed as the time after which no more fluctuations of reject rate can be observed. One thing to point out is that the fluctuations of reject rate can be smoothed out if we choose larger window sizes.

## 5. MULTI-FILE SYSTEM

In the previous section, we derived explicit expressions for the system capacity  $C(k)$  and the server-peer transition time  $k_0$  for a single-file system. In deriving these expressions, we used Eq.(1) to capture the increase in number of qualified peers in two consecutive time intervals. However, we cannot directly use Eq.(1) to

study the dynamics of a multi-file system because of the interactions among peers holding and/or requesting more than one file. To clarify, consider a peer that has received a file  $f_1$  in the past, i.e., it is considered a qualified peer for  $f_1$ . If that peer requests and receives another file  $f_2$ , it should not be counted as a qualified peer for both files because it may not have enough streaming capacity to serve both files at the same time. Intuitively, the rate of increase of the number of qualified peers will be smaller in a multi-file system than in a single-file system. Another problem is: when the growth of file-specific capacity are not well synchronized, we could also have long transition time. In this section, we analyze a multi-file system in which all files have the same length  $L$  and the same bit rate  $b$ . We first consider a simplified multi-file system model, for which we derive the optimal (i.e., shortest) server-peer transition time  $k_0$  for the system and the conditions to achieve this optimal value. We then study a general multi-file system by analyzing the impact of the assumptions made in the simplified model.

In the simplified multi-file system, we divide the whole system into  $F$  virtual subsystems, each of which deals with only one file. Each individual subsystem is assigned a fixed share  $N_f$  of the total server bandwidth  $N$ . In other words, we divide the server capacity into  $F$  private channels. Naturally, each subsystem has its own request rate  $\lambda_f$ . Immediately, we have

$$\sum_{f=1}^F N_f = N, \text{ and } \sum_{f=1}^F \lambda_f = \lambda. \quad (6)$$

We further assume that the one-file subsystems are independent, i.e. a peer that has acquired file  $f$  will request no other files and remains a qualified peer of subsystem  $f$  forever. The whole system can then be viewed as  $F$  independent subsystems sharing the total server bandwidth  $N$ . The simple model differs from the original model by two factors: private channeling of the server bandwidth to individual files, and lack of interactions among subsystems. We discuss the effects of these factors in Section 5.1 and Section 5.2, respectively.

It is easy to see that the growth of each subsystem capacity follows Eq.(1) with  $N$  replaced by  $N_f$  and  $\lambda$  by  $\lambda_f$ . Therefore, the server-peer transition time for any single-file subsystem (denoted as  $k_{0,f}$ ) can be obtained from Eq.(5) as follows:

$$k_{0,f} = \frac{\lg(\lambda_f L b) - \lg N_f}{\lg(1 + \frac{\alpha}{b})}. \quad (7)$$

Eq.(7) shows that the server-peer transition time in each subsystem depends only on the bandwidth allocation ( $N_f$ ) and the per-file request rate ( $\lambda_f$ ). Now we need to derive the system-level server-peer transition time  $k_0$  from those of the subsystems. We can easily see that different allocations of server bandwidth may result in different server-peer transition times. Instead of deriving general expressions for  $k_0$  as a function of  $N_f$ , we concentrate on the bandwidth allocations that lead to the optimal  $k_0$ . The problem of finding such allocation(s) can be formally stated as: for each media file  $f$ , how much server bandwidth is to be assigned ( $N_f$ ) given the request rate of that file ( $\lambda_f$ ) such that the system-level transition time ( $k_0$ ) is minimized. One important observation is that the system-level transition time is the maximum value among those of all subsystems. This

is because the whole system reaches the transition point only when all subsystems reach theirs. The problem can be further interpreted as an optimization subject to the constraints represented by Equations (6) and (7), with the objective function

$$\text{minimize } \max_{1 \leq f \leq F} \{k_{0,f}\}.$$

It is well-known [Chong and Zak 2001] that the solution for the above optimization is obtained when all  $k_{0,f}$  are the same, i.e.,

$$k_0 = k_{0,1} = k_{0,2} = \dots = k_{0,F}.$$

Applying Eq.(7) to the above solution, we get

$$\frac{\lambda_1 Lb}{N_1} = \frac{\lambda_2 Lb}{N_2} = \dots = \frac{\lambda_F Lb}{N_F} = \frac{\sum_{i=1}^F \lambda_i Lb}{\sum_{i=1}^F N_i} = \frac{Lb \sum_{i=1}^F \lambda_i}{N} = \frac{Lb\lambda}{N}.$$

Hence for any file  $f$ , the optimal choice of  $N_f$  is

$$N_f = \frac{\lambda_f}{\lambda} N, \quad f = 1, 2, \dots, F. \quad (8)$$

In other words, the share of server bandwidth assigned to each single-file subsystem has to be proportional to the request rate of that file to achieve optimal  $k_0$  at the system level. Now we can derive  $k_0$  from Eq.(7) and Eq.(8):

$$k_0 = \frac{\lg(\lambda Lb) - \lg N}{\lg(1 + \frac{\alpha}{b})}. \quad (9)$$

Note that the above equation is the same as Eq.(5). From Eq.(9) we can also get the number of qualified peers for file  $f$  at time  $k_0$ :

$$P_f(k_0) = \frac{N_f}{\alpha} \left( \frac{\lambda_f Lb}{N_f} - 1 \right) = \frac{\lambda_f Lb}{\alpha} - \frac{N_f}{\alpha}, \quad f = 1, 2, \dots, F. \quad (10)$$

### 5.1 Optimality of the Original System Model.

The above result is important since it shows that the simple model is optimal in terms of server-peer transition time when the bandwidth allocation follows Eq.(8). Let us go back to the original system model. In this model, no private channels are assigned to individual files. Instead, requests come at random and can be admitted to any server channel that is available. We call this *statistical multiplexing* of server capacity. This makes  $N_f$  a random variable instead of a constant. For any file  $f$ , we model the request arrivals as a Poisson process with rate  $\lambda_f$ . The following theorem shows that the original system model is stochastically optimal.

**THEOREM 5.1.** *In a multi-file hybrid streaming system that performs statistical multiplexing of server capacity, the expectation of the server bandwidth utilized in streaming file  $f$  is  $E[N_f] = \frac{\lambda_f}{\lambda} N$ .*

**PROOF.** The server bandwidth can be viewed as  $\frac{N}{b}$  channels, each of which can serve a streaming session. The  $F$  file-specific request streams can be viewed as a single Poisson stream with a fixed rate  $\lambda = \sum_{f=1}^F \lambda_f$ . Channel holding time for all requests is a constant  $L$  and requests do not stay in a waiting queue. With all these conditions, it follows that the CDN servers in our streaming system can be

mapped to an Erlang loss system with  $\frac{N}{b}$  service lines, arrival rate of  $\lambda$ , and service rate  $\frac{1}{L}$  [Cooper 1981].

In the aggregate stream, the probability that a single request is to file  $f$  is  $\frac{\lambda_f}{\lambda}$ . According to well-established results in queuing theory ([Cooper 1981], page 84), the probability of rejection (blocking) is the same for all file-specific streams in such systems. Therefore, for any non-blocked request, the probability that it is to file  $f$  is still  $\frac{\lambda_f}{\lambda}$ . Consider any  $\frac{N}{b}$  consecutive non-blocked requests in the aggregate stream, the number of requests to file  $f$  can be denoted as a random variable  $X_f$ , which follows a binomial distribution  $B(\frac{N}{b}, \frac{\lambda_f}{\lambda})$ . Therefore, the bandwidth consumed by file  $f$  is  $N_f = bX_f$ . It follows that  $E[N_f] = bE[X_f] = b\frac{N}{b}\frac{\lambda_f}{\lambda} = \frac{\lambda_f}{\lambda}N$ .  $\square$

From Theorem 5.1, we see that since  $E[N_f]$  gets the optimal bandwidth given by Eq.(8), the server-peer transition time for the statistical multiplexing system will approximately achieve the optimal  $k_0$  value in Eq.(9). The above proof requires familiarity with Erlang systems, a self-contained proof based on probability density functions of exponential distributions can be found in [Tu et al. 2005].

Theorem 5.1 only shows the expectation of  $N_f$  without considering the effects of the variance of  $N_f$  on  $k_0$ . We can use standard statistical tools to estimate  $k_0$  with the consideration of such variances. First of all, the variance of  $N_f$  is

$$\sigma^2 = b^2 \frac{N}{b} \frac{\lambda_f}{\lambda} \left(1 - \frac{\lambda_f}{\lambda}\right) = \frac{bN\lambda_f}{\lambda} \left(1 - \frac{\lambda_f}{\lambda}\right).$$

We now can analyze  $N_f$  using confidence intervals. If the random variable  $N_f$  falls into an 95% interval, say,  $N_f \in (E[N_f] - 0.05\sigma, E[N_f] + 0.05\sigma)$ , we get  $N_f \geq E[N_f] - 0.05\sigma = \frac{\lambda_f}{\lambda}N - 0.05\sigma$ . By Eq.(7), we have  $k_0 \leq \frac{\lg(\lambda_f Lb) - \lg(\frac{\lambda_f}{\lambda}N - 0.05\sigma)}{\lg(1 + \frac{\alpha}{b})}$ . This result gives an upper bound for  $k_0$  taking the variance of randomly distributed  $N_f$  into consideration. Since the effects of  $\sigma$  on  $k_0$  are diluted by the log function,  $k_0$  is not sensitive to the variance of  $N_f$ . As long as  $\sigma$  is relatively large (i.e.,  $\frac{bN\lambda_f}{\lambda}$  is not so small),  $k_0$  is very close to our result in Eq.(7).

## 5.2 Dependence Among Subsystems

In the analysis of a multi-file system, we assume that different subsystems grow independently. However, interactions exist among these virtual subsystems in the original model. As described earlier in this section, the problem comes from those peers that access more than one media object. It is difficult to quantify such interactions among media files. In this section, we give an upper bound of the level of these interactions. The following analysis shows that  $k_0$  is only slightly larger than the value given by Eq.(5).

We assume that any request to file  $f$  comes uniformly from all  $M$  potential clients, i.e., there is no tendency that a peer already holding file A has a better chance to ask for file B. Let us go back to the analysis of multi-file systems, reconsider Eq.(1), and take the peer interactions into account, we have:

$$P_f(k+1) = P_f(k) + \beta_{k,f} \left( \frac{N_f}{b} + P_f(k) \frac{\alpha}{b} \right), \quad 0 \leq k \leq k_0 \quad (11)$$

where  $\beta_{k,f}$  ( $0 < \beta_{k,f} \leq 1$ ) is a coefficient for the ‘valid’ proliferation in the subsystem

of file  $f$ . This means that  $\beta_{k,f}$  is the probability that peers in this subsystem hold only file  $f$  during time interval  $k$ . We call such peers as *valid peers* of file  $f$ . If a peer holds other media file(s) when it acquires file  $f$ , it is called an *invalid peer* of media  $f$ . Suppose at time  $k$ ,  $P_f(k)$  is the number of valid peers. By the assumption of uniformly-distributed requests, the probability of getting a request from a peer that holds another file  $g$  is at most  $\frac{P_g(k)}{M}$ . Since  $g$  could be any of the  $F - 1$  files other than  $f$ , the total probability of having an invalid peer (denoted by  $\delta_{k,f}$ ) is

$$\delta_{k,f} \leq \sum_{g \neq f} \frac{P_g(k)}{M},$$

which captures the portion of peers that should not be counted as contributors in the subsystem of file  $f$ . At any time up to  $k_0$ , Eq.(10) gives an upper bound for the number of valid peers in any subsystem  $g$ , and we have

$$\sum_{g \neq f} P_g(k) \leq \sum_{g=1}^F \frac{\lambda_f Lb}{\alpha} - \frac{\lambda_f N}{\alpha \lambda} \left( \frac{\lambda_f Lb}{N} - 1 \right) \leq \frac{\lambda Lb}{\alpha} - \frac{N}{\alpha},$$

which is independent of the total peer population  $M$ . Thus,  $\delta_{k,f} \leq \frac{\lambda Lb - N}{M\alpha}$ . Now, the probability of having valid peers for file  $f$  is  $\beta_{k,f} = 1 - \delta_{k,f} \geq 1 - \frac{\lambda Lb - N}{M\alpha}$ . Note that if the pool size of peers is large enough, i.e., the request rate is small compared to  $M$ , we have  $\beta_{k,f} \geq 1 - \frac{\lambda Lb - N}{M\alpha} \approx 1$ . From Eq.(11), we get

$$P_f(k+1) \geq P_f(k) + \left( 1 - \frac{\lambda Lb - N}{M\alpha} \right) \left( \frac{N_f}{b} + P_f(k) \frac{\alpha}{b} \right).$$

Following the same procedures as in the derivation of Eq.(9) and Eq.(10) and setting  $\beta = 1 - \frac{\lambda Lb - N}{M\alpha}$ , we obtain  $P_f(k) \geq \frac{N_f}{\alpha} \left[ \left( 1 + \frac{\alpha\beta}{b} \right)^k - 1 \right]$ , which leads to  $k_0 \leq \frac{\lg(\lambda Lb) - \lg N}{\lg(1 + \frac{\alpha\beta}{b})}$ .

## 6. IMPACT OF PEER FAILURE

P2P systems are intrinsically dynamic [Saroiu et al. 2003]. A major difference between a peer and a server is that a peer's commitment to the community is not guaranteed: it may leave the network at any time. In this section, we study the effects of peer failure on the capacity growth of our media streaming system. Peer failure in our analysis means that a peer leaves the system permanently [Bhagwan et al. 2003]. We start by presenting a simple peer failure model that is based on experimental studies performed by other researchers. Then we present a general peer failure model that considers an arbitrary distribution for peer lifespan.

### 6.1 Simple Model for Peer Failure

In this failure model, we assume that at the end of each streaming period (i.e., generation), the number of surviving qualified peers is proportional to the number of surviving qualified peers at the beginning of that streaming period. The proportionality factor is called the *survival rate* and is denoted by  $\gamma$  ( $\gamma < 1$ ). We discuss how to determine  $\gamma$  later in this section.

At generation  $k + 1$ , the number of inherited qualified peers from generation  $k$  is  $\gamma P(k)$ . Consider the case for the single-file system, Eq.(1) becomes

$$P(k + 1) = \gamma P(k) + \frac{N}{b} + \gamma P(k) \frac{\alpha}{b}, \quad 0 \leq k \leq k_0. \quad (12)$$

Rewriting the above equation, we have

$$P(k + 1) + \frac{N}{b\theta} = \left( P(k) + \frac{N}{b\theta} \right) \gamma \left( 1 + \frac{\alpha}{b} \right),$$

where  $\theta$  is the new capacity growth factor and  $\theta = \gamma(1 + \frac{\alpha}{b}) - 1 \neq 0$ . Then Eq.(2) and Eq.(5) become

$$P(k) = \frac{N}{b\theta} \left[ \gamma^k \left( 1 + \frac{\alpha}{b} \right)^k - 1 \right] = \frac{N}{b} \cdot \frac{\gamma^k \left( 1 + \frac{\alpha}{b} \right)^k - 1}{\gamma \left( 1 + \frac{\alpha}{b} \right) - 1} \quad (13)$$

and

$$k_0 = \frac{\lg \left( \frac{b(\gamma-1) + \gamma\alpha}{\alpha\gamma} \left( \frac{\lambda L b}{N} - 1 \right) + 1 \right)}{\lg \gamma \left( 1 + \frac{\alpha}{b} \right)}, \quad (14)$$

respectively. Note that Eq.(2) and Eq.(5) are special cases of Eq.(13) and Eq.(14) when  $\gamma = 1$ . To guarantee positive growth of the system capacity, we must have  $\theta > 0$  and therefore  $\gamma > \frac{b}{\alpha + b}$ .

Once we have Eq.(14), we can follow the same analysis as in Section 5 to derive the upper bound for multi-file systems and get  $\frac{\lambda_1 L b}{N_1} = \frac{\lambda_2 L b}{N_2} = \dots = \frac{\lambda_F L b}{N_F} = \frac{\sum_{i=1}^F \lambda_i L b}{\sum_{i=1}^F N_i} = \frac{L b \sum_{i=1}^F \lambda_i}{N} = \frac{L b \lambda}{N}$ . That is, we have the optimal choice of  $N_f$  as  $N_f = \frac{\lambda_f}{\lambda} N$  ( $f = 1, 2, \dots, F$ ), which is the same as in Eq.(8). Thus, we get the same equation as Eq.(14) for the system-level transition time of a multi-file system with peer failures. Once we have the above equations, the other results in Section 5 can be derived accordingly.

**6.1.1 Computing the survival rate  $\gamma$ .** To determine the survival rate  $\gamma$ , we associate with each qualified peer a random variable  $X$  to model its *lifespan*. Assuming peers fail independently, then the survival rate  $\gamma$  can be interpreted as the conditional probability:

$$\gamma = Pr\{X \geq T + L \mid X > T\}, \quad (15)$$

where  $T$  is the starting time of any streaming period  $k$ . Generally, it is difficult to solve Eq.(12) using Eq.(15) when the peer lifespan follows an arbitrary statistical distribution. The reason is that the above probability for any individual peer depends on its age  $T$ . In other words,  $\gamma$  is a variable that is related to  $k$ . Two large-scale measurement studies analyzed the lifespan of peers ([Sariou et al. 2003] and [Bustamante and Qiao 2003]). According to [Sariou et al. 2003], the lifespan of peers approximately follows an exponential distribution. Since the exponential distribution is memoryless, the probability for any peer to live beyond time  $T + t$  given it is alive at time  $T$  is  $e^{-tq}$ , where  $1/q$  is the average lifespan of all peers. Thus, in our case,  $\gamma = e^{-Lq}$ .

The measurement study in [Bustamante and Qiao 2003] indicates that a long-tail Pareto distribution is a better fit for the lifespan data collected from more

than 500,000 peers. Since Pareto distribution is not memoryless, computing  $\gamma$  from Eq.(15) is not easy. However, it is shown in [Feldmann and Whitt 1997] that long-tail distributions can accurately be approximated by a weighted sum of a small number of exponential distributions over a finite time interval. The maximum peer lifespan can be assumed to be a sufficiently large (e.g., 100 days) but finite value for all practical purposes. Therefore, we can approximate the distribution of the peer lifespan as  $\sum_{i=1}^m w_i e^{-\mu_i t}$  where the parameters  $m, w_i$  and  $\mu_i$  are estimated using the recursive algorithm described in [Feldmann and Whitt 1997]. Using this approximate distribution for peer lifespan in Eq.(15), the survival rate is given by:  $\gamma = \sum_{i=1}^m w_i e^{-\mu_i L}$ .

## 6.2 General Model for Peer Failure

The previous section presented a peer failure model for two commonly conceived distributions for peer lifespan. Although these two distributions are corroborated by extensive measurement studies, they are system and environment specific. Therefore, they may not be applicable to other P2P systems, or their accuracy may degrade under different conditions. In this section, we develop a more general peer failure model that is not restricted to particular peer lifespan distributions.

With a general lifespan distribution, we lose the nice feature of representing the survival probability within any time interval as a constant. What we can do is to divide the continuous *peer age* (i.e., the length of time since a peer becomes online) into discrete *age classes* and associate a survival probability  $p$  with each age class. In our analysis, we use age classes with length  $L$ . Without loss of generality, we ignore peers with age more than  $m$ , and  $m < k_0$ . We denote the survival probability from age  $k$  to age  $k+1$  as  $p_k$ . Suppose we obtain the probability density function of peer lifespan  $f(x)$  from measurement studies. Based on Eq.(15), we have  $p_k = \frac{\int_{k+1}^{\infty} f(x) dx}{\int_k^{\infty} f(x) dx}$ . The overall survival rate  $\gamma$  at time  $k$  is thus determined by the *age structure* of all  $P(k)$  qualified peers, i.e.,

$$\gamma = [x_0, x_1, \dots, x_m][p_0, p_1, \dots, p_m]^T,$$

where  $x_i$  is the percentage of peers of age  $i$  among the  $P(k)$  qualified peers.

Following the same strategy as in Section 4, we develop a model to project the number of qualified peers from time  $k$  to  $k+1$ . Define  $n_{xk}$  as the number of peers with age  $x$  at generation  $k$ , where  $x \geq 0$ , and  $k \geq 0$  are integers. We have the following relations between different age groups in the single-file system:

$$\begin{aligned} \frac{N}{b} + \frac{\alpha}{b} \sum_{x=0}^m n_{xk} &= n_{0k+1}, & k = 0, 1, \dots, k_0 - 1, \\ p_x n_{xk} &= n_{x+1k+1}, & x = 0, 1, \dots, m - 1, \text{ and } k = 0, 1, \dots, k_0. \end{aligned}$$

The first relation shows that the number of qualified peers of age 0 at time  $k+1$  is the sum of those generated by servers and by peers of all other age classes. The second relation shows that the peers of age  $x+1$  at time  $k+1$  are those of age  $x$  at time  $k$  and survived through time period  $k$  with probability  $p_x$ . Employing matrix notation, the system capacity can be expressed as

$$\vec{B} + \mathbf{A}\vec{n}_k = \vec{n}_{k+1}, \quad (16)$$

where

$$\vec{B} = \begin{bmatrix} \frac{N}{b} \\ 0 \\ \vdots \\ 0 \end{bmatrix}, \quad \vec{n}_k = \begin{bmatrix} n_{0k} \\ n_{1k} \\ \vdots \\ n_{mk} \end{bmatrix}, \quad \vec{n}_{k+1} = \begin{bmatrix} n_{0k+1} \\ n_{1k+1} \\ \vdots \\ n_{mk+1} \end{bmatrix}, \quad \text{and } \mathbf{A} = \begin{bmatrix} \frac{\alpha}{b} & \frac{\alpha}{b} & \cdots & \frac{\alpha}{b} & \frac{\alpha}{b} \\ p_0 & 0 & \cdots & 0 & 0 \\ 0 & p_1 & \cdots & 0 & 0 \\ \vdots & \vdots & \ddots & \vdots & \vdots \\ 0 & 0 & \cdots & p_{m-1} & 0 \end{bmatrix}.$$

Note that the above formula has a similar form as Eq.(1). Set  $p_{(k)} = p_0 p_1 \cdots p_k$  ( $k \geq 0$ ) and  $p_{(-1)} = 1$ . We also define the following column vector

$$\vec{v} = \frac{N}{-b + \alpha \sum_{k=0}^m p_{(k-1)}} [1, p_{(0)}, p_{(1)}, \dots, p_{(m-1)}]^T.$$

We explain more about this vector later. For vector  $\vec{v}$ , it can be verified that  $\mathbf{A}\vec{v} - \vec{v} = \vec{B}$ . Plugging it into Eq.(16), we obtain

$$\vec{n}_{k+1} + \vec{v} = \mathbf{A}(\vec{n}_k + \vec{v}), \quad \vec{n}_0 = \vec{0}. \quad (17)$$

Solving the above equation, we get:

$$\vec{n}_k = (\mathbf{A}^k - I)\vec{v}, \quad k = 1, 2, \dots, k_0, \quad (18)$$

where  $I$  is the  $(m+1) \times (m+1)$  identity matrix. This can be viewed as a matrix counterpart of Eq.(2). We now can see that the purpose of introducing vector  $\vec{v}$  is to get the nice form shown in Eq.(17) such that  $\vec{n}_k$  can be solved as an exponential function of  $k$ .

Now let us discuss under what conditions the system capacity grows positively. For convenience, let  $\psi = -1 + \frac{\alpha}{b} \sum_{k=0}^m p_{(k-1)}$ , which immediately gives  $\vec{v} = \frac{N}{b\psi} [1, p_{(0)}, p_{(1)}, \dots, p_{(m-1)}]^T$ . Obviously, the elements in  $\vec{v}$  should all be positive to achieve positive capacity growth. Therefore, we must have  $\psi > 0$ . We may also see that, to guarantee positive growth, the largest eigenvalue of  $\mathbf{A}$  should be greater than 1.

To find the server-peer transition time  $k_0$  (assuming the above conditions hold such that the capacity grows positively), we need to solve

$$\frac{N}{b} + \frac{\alpha}{b} \sum_{x=0}^m n_{xk_0} = \lambda L,$$

or equivalently, solve

$$\frac{N}{b} + \frac{\alpha}{b} (\mathbf{A}^{k_0} - I)\vec{v} = \lambda L.$$

Divide both sides by  $\frac{N}{b}$ , we obtain

$$1 + \frac{1}{\psi} \frac{\alpha}{b} (\mathbf{A}^{k_0} - I) [1, p_{(0)}, p_{(1)}, \dots, p_{(m-1)}]^T = \frac{\lambda b L}{N}. \quad (19)$$

Since the system grows exponentially, the left-hand side of Eq.(19) is proportional to the increased population of the system, it is an increasing function of  $k_0$ , and we

will have a unique  $k_0$  satisfying Eq.(19). Unfortunately, we could not find a simple explicit expression for  $k_0$ . Instead, we can calculate  $k_0$  numerically. Moreover, since the right-hand side depends on the ratio of the bandwidth and the request rate rather than their absolute values, the solution of  $k_0$  will depend only on this ratio. Hence, if we generalize the single-file solution to multi-file systems, where each media object has its own request rate  $\lambda_f$ , we will have the same result as in Eq.(8), i.e. the optimal bandwidth is proportional to the request rate.

## 7. OTHER EXTENSIONS

### 7.1 Acceleration of Capacity Growth

In the previous sections, we assume that a peer can only serve others after it finishes receiving the entire stream. In practice, it is feasible to allow peers to start serving others after receiving the first few blocks of the media file. Formally, we set a delay  $d$  ( $d \leq L$ ) after which a requesting peer in a streaming session can serve as a supplying peer in a new session. In this section, we study how the inter-session delay  $d$  affects system performance.

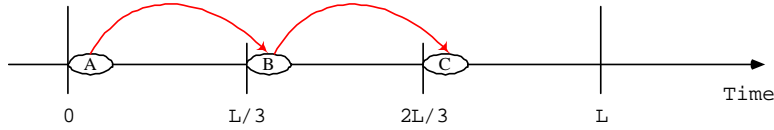


Fig. 4. Streaming sessions initiated in a generation when  $d = L/3$ .

For simplicity, we only consider the situation of  $d = L/n$  where  $n$  is a positive integer. When  $n$  is not an integer, we can estimate  $k_0$  using the two neighboring integers of  $n$ . Revisiting the arguments used to generate Eq.(1) in Section 4, an important observation is: within one streaming period, a newly started session will have the chance to start  $n - 1$  rounds of new sessions. Figure 4 shows an example of  $n = 3$  and we use cluster  $A$  to represent the chunk of sessions initiated at the beginning of a streaming period. The requesting peer in a session in cluster  $A$  could be a supplying peer in a new session that starts in the beginning of time interval  $[\frac{L}{3}, \frac{2L}{3}]$  (cluster  $B$ ). The requesting peer of a cluster  $B$  session can in turn be a supplying peer in a session in cluster  $C$ . On average, one session in cluster  $A$  can give rise to  $\frac{\alpha}{b}$  sessions in cluster  $B$  and  $\frac{\alpha}{b} \cdot \frac{\alpha}{b} = \frac{\alpha^2}{b^2}$  sessions in cluster  $C$ . Knowing this, the number of sessions initiated in the period shown in Figure 4 is  $|A| + |B| + |C| = |A|(1 + \frac{\alpha}{b} + \frac{\alpha^2}{b^2})$  where  $|A|$ ,  $|B|$ ,  $|C|$  are the numbers of sessions in cluster  $A$ ,  $B$ , and  $C$ , respectively. Generalizing this idea, Eq.(1) can be written as:

$$P(k+1) - P(k) = \left( \frac{N}{b} + P(k) \frac{\alpha}{b} \right) \left( 1 + \frac{\alpha}{b} + \frac{\alpha^2}{b^2} + \dots + \frac{\alpha^{n-1}}{b^{n-1}} \right) \quad (20)$$

with  $0 \leq k \leq k_0$  and  $P(0) = 0$ . Let  $\Phi_n = 1 + \frac{\alpha}{b} + \frac{\alpha^2}{b^2} + \dots + \frac{\alpha^{n-1}}{b^{n-1}}$ . Similar to the derivation of Eq.(2), we obtain

$$P(k) = \frac{N}{\alpha} \left[ \left( 1 + \frac{\alpha}{b} \Phi_n \right)^k - 1 \right].$$

The server-peer transition time becomes

$$k_0 = \log_{(1+\frac{\alpha}{b}\Phi_n)} \left( \frac{\lambda L b}{N} \right) = \frac{\lg(\lambda L b) - \lg N}{\lg(1 + \frac{\alpha}{b}\Phi_n)}. \quad (21)$$

Comparing this with Eq.(5), we see that the improvement is significant because the system capacity growth factor increases to  $1 + \frac{\alpha}{b}\Phi_n$  while other factors remain unchanged. A smaller delay  $d$  leads to a smaller  $k_0$  value. However, this does not mean it is always better to choose a smaller  $d$  (i.e., a larger  $n$ ) value. Since we have  $\frac{\alpha}{b} < 1$  in practice,  $k_0$  converges rapidly as  $n$  increases: it is well-known that for  $\Phi_n = \frac{1 - (\frac{\alpha}{b})^n}{1 - \frac{\alpha}{b}}$ , we have  $\lim_{n \rightarrow \infty} \Phi_n = \frac{b}{b - \alpha}$ . It follows that we get  $\lim_{n \rightarrow \infty} k_0 = \frac{\lg(\lambda L b) - \lg N}{\lg(1 + \frac{\alpha}{b - \alpha})}$ . From the point of view of streaming protocol design, an excessively short delay is also infeasible: there will inevitably be some delays in setting up the network connections, and some buffer time is needed for maintaining QoS in any streaming sessions.

## 7.2 General Multi-file System

In the analysis of multi-file systems (Section 5), we assume that all media files require the same bandwidth  $b$  and have the same length  $L$ . Our analysis can be generalized to media files with different bandwidth requirements and streaming lengths. Assume that a media file  $f$  requires bandwidth  $b_f$ , and streaming length  $L_f$ . Then the proliferation of each subsystem capacity follows Eq.(1) with  $N$  replaced by  $N_f$  and  $b$  by  $b_f$ . Therefore, the server-peer transition time for any single-file subsystem ( $k_{0,f}$ ) can be obtained from Eq.(5) as:

$$k_{0,f} = \frac{\lg(\lambda_f L_f b_f) - \lg N_f}{\lg(1 + \frac{\alpha}{b_f})}. \quad (22)$$

Note that the time unit for every subsystem is its streaming length  $L_f$ , so that the objective function of the optimization problem becomes:

$$\text{minimize } \max_{1 \leq f \leq F} \{L_f k_{0,f}\}. \quad (23)$$

If we allow  $k_{0,f}$  to have continuous solutions, the solution of the above optimization problem is achieved when  $L_f k_{0,f}$  are equal to each other for each  $f$ . Let  $T_0$  be the optimal transition time, we have  $T_0 = k_{0,f} L_f, \forall f$ , which is the same as

$$T_0 = \frac{\lg(\lambda_1 L_1 b_1) - \lg N_1}{\lg(1 + \frac{\alpha}{b_1})} L_1 = \frac{\lg(\lambda_2 L_2 b_2) - \lg N_2}{\lg(1 + \frac{\alpha}{b_2})} L_2 = \dots = \frac{\lg(\lambda_F L_F b_F) - \lg N_F}{\lg(1 + \frac{\alpha}{b_F})} L_F$$

where  $N_1, N_2, \dots, N_F$  are the unknowns. With the condition  $\sum_{f=1}^F N_f = N$ , we could solve  $N_1, N_2, \dots, N_F$  by iteration methods. That is, we first solve  $T_0$  by representing  $N_f$  through  $T_0$  and plugging it into the sum condition. Since  $N_f = \lambda_f L_f b_f \left( \frac{b_f}{b_f + \alpha} \right)^{T_0/L_f}$ , we have

$$\sum_{f=1}^F \lambda_f L_f b_f \left( \frac{b_f}{b_f + \alpha} \right)^{T_0/L_f} = N.$$

The left-hand side of the above equation monotonically decreases about  $T_0$ . This means the equation has a unique root. There are many quick iteration techniques to solve  $T_0$  such as the bisection method, Newton's method, and the secant method, details of which can be found in general numerical analysis texts such as [Burden and Faires 2001]. Note our original system model is not optimal under such conditions therefore we have to assign private channels to files based on the solution of the above equation to achieve the shortest  $T_0$ .

*Remark 7.1.* The above analysis can be further generalized to the scenario where each media file attracts a different group of peers with different bandwidth contributions (i.e., the quantity  $\alpha$  in Eq.(22) is replaced by a file-specific item  $\alpha_f$ ). Under such changes,  $T_0$  can still be solved by the same iteration methods.

## 8. EXPERIMENTAL RESULTS

We study the dynamics of the proposed hybrid media streaming system by extensive simulations. We implement our media streaming simulator using the Tool Command Language (TCL)<sup>9</sup>.

Unless specified otherwise, the example system contains a pool of 200,000 peers ( $M = 200,000$ ). The playback bit rate for all video objects is  $b = 800Kbps$  and length is one hour ( $L = 3,600$ , basic time unit is *second*). Bandwidth contribution of peers is: 5% of the peers with 800Kbps, 10% with 400Kbps, 55% with 200Kbps, and 30% with 100Kbps, which translates into an  $\frac{\alpha}{b}$  value of 0.275. System receives requests at a rate ( $\lambda$ ) of 1 request per second. Total server bandwidth is 480Mbps. Due to space limit, we only present the most important experimental results.

### 8.1 Dynamics of Single-File Systems

In Figure 5, various metrics of the simulated system are plotted. After a short initial stage, server bandwidth usage (Figure 5a) is close to the maximum value all the time. We plot reject rates resulted from two window sizes, 8000 seconds and 1000 seconds, in Figure 5c. For the one with smaller window size, reject rate fluctuates between zero and one. These fluctuations almost disappear in the experiment using windows of size 8000. For both experiments, the reject rate stays at zero after 8.06 hours. According to Section 4.0.1, the time point 8.06 can be regarded as the  $k_0$  value for this experiment as no fluctuations occur afterwards. We also test windows with other sizes but the same  $k_0$  value is observed.

The growth of system capacity is illustrated by the change of total number of qualified peers (Figure 5b) and bandwidth contributions of these peers (Figure 5d). Both peer number and peer bandwidth show geometric growth at the first 8 hours and linear growth afterwards. One thing to point out is that the curves for system capacity growth are not smooth. They tend to appear as step functions of time, as illustrated by the small graph in Figure 5. The height of steps increases as time goes by, thus an exponential growth is achieved. From Figure 5d we can also see that the system capacity reaches the requested bandwidth at about the 8th hour, which confirms our conclusion about transition time drawn from reject rate data.

<sup>9</sup><http://tcl.sourceforge.net>

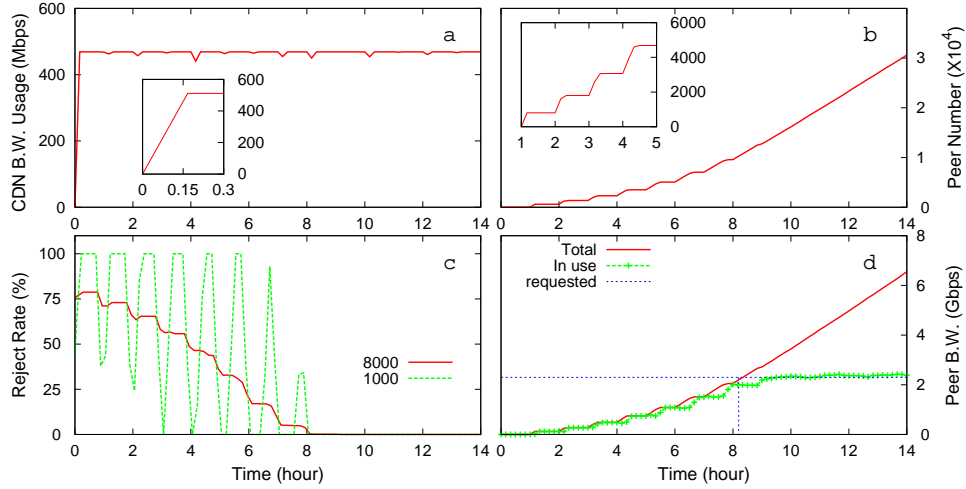


Fig. 5. Performance of a typical hybrid media streaming system. a. Bandwidth usage of CDN servers; b. Number of qualified peers; c. System reject rate; d. Peer capacity.

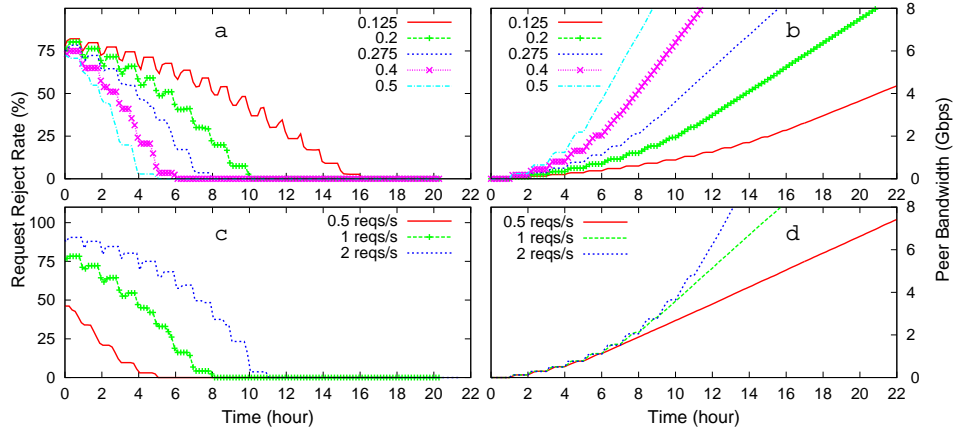


Fig. 6. System performance under different capacity growth factors (a, b) and request rates (c, d). a,c: Smoothed system reject rate; b,d: Peer bandwidth.

Peer bandwidth usage first increases and then stabilizes (after transition point) at exactly the same level with the requested bandwidth.

8.1.1 *Effects of peer bandwidth contribution and request rate.* The impact of parameters  $\frac{\alpha}{\beta}$  and  $\lambda$  on performance is also investigated. Figure 6a and 6b show the reject rate and total peer bandwidth under different choices of  $\alpha$  while all other parameters remain unchanged. The legends in Figure 6a and Figure 6b indicate the  $\frac{\alpha}{\beta}$  values of individual simulations. A four-fold increase of  $\frac{\alpha}{\beta}$  (from 0.125 to 0.5) significantly shortened the server-peer transition time from 16 hours to 5 hours. This shows that  $k_0$  is almost linearly related to  $\frac{\alpha}{\beta}$  (recall Remark 4.1).

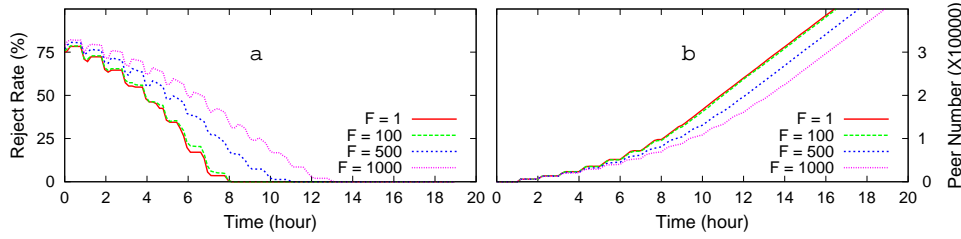


Fig. 7. System performance under different number of media files. a. Smoothed system reject rate; b. Number of qualified peers.

A similar set of experiments are designed to study the impact of system request rate ( $\lambda$ ) on  $k_0$ . The results for three request rates, 0.5, 1, and 2 requests per second, are shown in Figures 6c and 6d. The value of  $k_0$  observed increases as the request rate increases. However, the change of  $k_0$  due to the change of  $\lambda$  is less dramatic than that caused by the change of  $\frac{\alpha}{b}$ . When  $\lambda$  increases 20 times to 10 requests/second, a  $k_0$  of 17.27 hours was obtained (data not plotted). The effects of streaming length ( $L$ ) and bitrate ( $b$ ) are similar to those of request rate (data not shown).

## 8.2 Performance of Multi-file Systems

As specified in Section 5, the theoretical value of the server-peer transition time  $k_0$  in a multi-file environment is the same for a single-file system. Figure 7 shows how the system performs under different  $F$  values. First of all, we can see that the results for experiments with total file number 1 and 100 are almost identical. In this set of experiments, the observed  $k_0$  value does not change until the total number of files goes beyond 120.

Table II. Storage usage of peers at transition time

Experiment	$k_0$ (h)	# of media files stored				$\beta$
		1	2	3	4	
$F = 1$	8	10895	0	0	0	1.000
$F = 50$	8	10791	21	0	0	0.998
$F = 100$	8	10678	21	0	0	0.998
$F = 250$	9	11268	31	0	0	0.997
$F = 500$	11	13808	89	0	0	0.994
$F = 1000$	13	14896	196	1	0	0.987

However,  $k_0$  is found to be greater than the ideal value when  $F$  further increases (Fig 7a). According to Section 5, two factors could account for the long transition time in a multi-file system: (i) peers that acquired multiple files, and (ii) lack of synchronization in the growth of per-file capacity. We investigate the effects of the first factor in the same set of experiments by recording the storage usage of qualified peers. In Table II, the number of qualified peers at transition time is listed by their storage consumption. For example, there are 11268 peers holding one media file (valid peer) and 31 peers holding two files for the simulation with 250 files. The

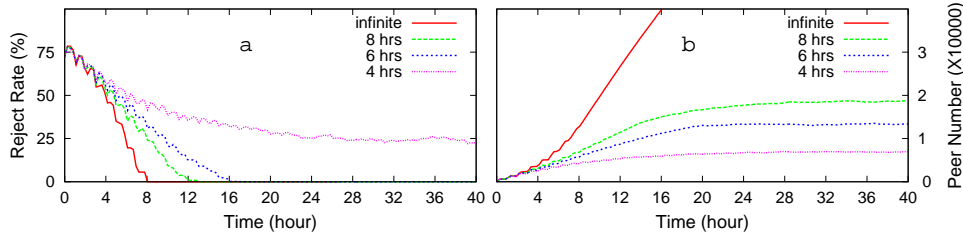


Fig. 8. Effects of peer failure on system dynamics. a. Smoothed system reject rate; b. Total number of qualified peers.

$\beta$  values in the last column are ratios of the number of valid peers to all qualified peers, which can be viewed as the lower bound of  $\beta_{k,f}$  in Eq.(11). All  $\beta$  values shown are very close to 1.0. Another conclusion we may draw from Table II is that the space contribution of peers can be made minimal without affecting system performance.

Now it is clear that factor (ii) above accounts for the degraded performance. According to Section 5.1, when  $F$  is large,  $\frac{bN\lambda f}{\lambda}$  is small and  $k_0$  deviates from theoretical value. In other words, the average number of sessions allocated to each file ( $\frac{N}{Fb}$ ) cannot be too small. Another way to interpret this is: when  $\frac{N}{Fb}$  is too small (e.g.  $F = 500$  in Fig 7), there is no guarantee that each file can occupy at least one server channel. Hence, the files take turns in using the server bandwidth and transition is delayed. For the above experiments, we see that  $\frac{N}{Fb}$  has to be at least 5 for the system to get near-optimal transition time.

### 8.3 Systems with Peer Failures

The introduction of finite peer lifespans significantly reduces the speed of system proliferation (Figure 8). We experiment with three simulations with different average peer lifespan – eight, six and four hours. In all tests, peer lifespan is exponentially distributed. A system with no peer failures (i.e. infinite peer lifespan) is used as control. As the average lifespan of peers increases, the reject rate drops more dramatically (Figure 8a) and the system accomplishes server-peer transition faster. For the system with average lifespan of 4.0 hours, the peers fail too early to serve other peers so that it never reaches a transition point. The above results are confirmed by capacity growth of all tested systems plotted in Figure 8b. For the systems simulated, the calculated threshold value of survival rate  $\gamma$  to guarantee positive capacity growth is 0.7843, which also means the peers should have an average lifespan of at least 4.12 hours.

### 8.4 Service Acceleration

We verify our conclusions about service acceleration (Section 7.1) by allowing requesting peers to act as supplying peers before the whole media stream is delivered. We test inter-session delays with different values (from  $L/5$  to  $L/2$ , and  $L$  as the control). From Figure 9, we can see that the usage of inter-session delays shorter than  $L$  does accelerate the server-peer transition:  $k_0$  decreases from 8.0 to about 6.0 when delay changes from  $L$  to  $L/2$ . Further decrease of  $k_0$  can also be observed

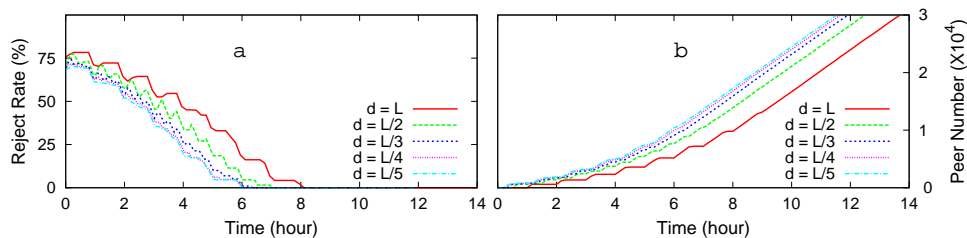


Fig. 9. System under different inter-session delays. a. Smoothed system reject rate; b. Total number of qualified peers.

when  $d$  gets even smaller. However, this effect on  $k_0$  quickly diminishes: the results of  $d = L/4$  and  $d = L/5$  are almost identical. We test different sequences of random inputs and very similar results are obtained and the  $k_0$  values observed match closely to the theoretical value given by Eq.(21)(data not shown).

## 9. CONCLUSIONS AND FUTURE WORK

In this paper, we studied the capacity growth of P2P media streaming systems using a discrete-time analytical model. The capacity is defined as the total streaming bandwidth available from both servers and peers that previously acquired the media files. Based on the analytical model, we found that the capacity of such systems increases exponentially with time. Knowing the exact pattern of the system capacity growth enabled us to determine the moment at which the streaming load can be shifted from servers to peers. We obtained explicit expressions to determine this moment, which we call the server-peer transition time  $k_0$ . The server-peer transition time can be used by the system operator to decide when to reallocate server resources. We analyzed the capacity and server-peer transition time for single- and multi-file streaming systems. We showed that the equations derived for single-file systems can approximate the behavior of multi-file systems, within some boundary conditions.

We extended our analysis to quantify the effects of peer failures on the system performance. In particular, we model the unreliability and limited commitment of peers to the system by a *lifespan* random variable. We derived explicit expressions for the server-peer transition time using two commonly-known lifespan distributions in the literature: exponential and Pareto. Furthermore, we considered a general peer failure model in which the lifespan could follow any arbitrary distribution. Although we did not obtain explicit expressions in this case, we showed how the solution can be computed using simple numerical methods. In addition, we conducted extensive simulation experiments which: (i) validated our analytical conclusions, and (ii) studied the effects of changing several parameters, e.g., request rate, average peer bandwidth contribution, and average peer lifespan on system performance.

Finally, our results from the analysis and the simulation experiments leads to better understanding of the operation of P2P media streaming systems. To that end, we have the following comments and suggestions for designers of P2P media streaming systems:

1. The system performance is most sensitive to the capacity growth factor, which is

the average peer bandwidth contribution ( $\alpha$ ) divided by the bandwidth required to stream the media file ( $b$ ). Therefore, we should concentrate on maintaining a large  $\frac{\alpha}{b}$  value. One idea is to give higher priorities to peers with higher bandwidth contributions. Specifically, we could reserve some server bandwidth for high-capacity peers to enable them to get early admission to the system;

2. Peers receiving a media file should be allowed to serve others before receiving the entire file. However, a receiving peer does not need to become a serving peer too early in the session. As a rule of thumb: a delay of about one-third of the session length would yield better performance in terms of faster system capacity growth rates;
3. Peer failure negatively affects the system capacity by decreasing the capacity growth factor. Thus, maintaining a sufficiently large P2P community is the key to success. Incentive mechanisms could be used to encourage peers to stay longer in the system.
4. System performance can deteriorate when too many media files are introduced in the system. To some extent, this may be mitigated by synchronizing the growth of file-specific subsystems using private channels, especially when files are of different lengths and bitrates.

This study can be extended in several directions. For example, it could be interesting to analyze the strategies proposed above (e.g., fast track channels for high-capacity peers and providing incentives for peers to stay longer) and how these strategies enhance system performance. Since the focus of our analysis was on the early stages of system operation, another extension can be studying the system dynamics after the server-peer transition point. At the individual peer level, we may need to design file replacement policies especially when peers request many files and have limited storage capacity. It is important to design these replacement policies with minimal or no global information about other peers in the system. Other possible research directions include QoS management and handling security and integrity concerns in P2P media systems.

## REFERENCES

- BHAGWAN, R., SAVAGE, S., AND VOELKER, G. 2003. Understanding availability. In *Proceedings of 2nd International Workshop on Peer-to-Peer Systems (IPTPS)*.
- BILIRIS, A., CRANOR, C., DOUGLIS, F., RABINOVICH, M., SIBAL, S., SPASTCHECK, O., AND STURM, W. 2002. CDN brokering. *Journal of Computer Communications* 25, 4 (March), 393–402.
- BURDEN, R. AND FAIRES, J. D. 2001. *Numerical Analysis*. Brooks/Cole Publishing.
- BUSTAMANTE, F. AND QIAO, Y. 2003. Friendships that last: Peer lifespan and its role in p2p protocols. In *Proceedings of International Workshop on Web Content Caching and Distribution*.
- CHONG, E. K. P. AND ŽAK, S. H. 2001. *An Introduction to Optimization*. John Wiley & Sons, New York.
- COOPER, R. B. 1981. *Introduction to Queueing Theory*. North Holland, New York.
- CROWCROFT, J. AND PRATT, I. 2002. Peer to Peer: peering into the future. In *Networking Tutorials*. 1–19.
- DABEK, F., KAASHOEK, M. F., KARGER, D., MORRIS, R., AND STOICA, I. 2001. Wide-area cooperative storage with CFS. In *Proceedings of ACM Symposium on Operating Systems Principles*. 202–215.
- FELDMANN, A. AND WHITT, W. 1997. Fitting mixtures of exponentials to long-tail distributions to analyze network performance models. In *Proceedings of IEEE INFOCOM*. 1096–1104.
- ACM Transactions on Multimedia Computing, Communications, and Applications, Vol. V, No. N, May 2005.

- FRANCIS, P., JAMIN, S., JIN, C., JIN, Y., RAZ, D., SHAVITT, Y., AND ZHANG, L. 2001. IDMaps: A global internet host distance estimation service. *IEEE Transactions on Networking* 9, 5 (October), 525–540.
- GOLLE, P., K. LEYLTON-BROWN, AND MIRONOV, I. 2001. Incentives for sharing in peer-to-peer networks. In *Proceedings of ACM Conference on Electronic Commerce (EC)*. 264–267.
- HEFEEDA, M., BHARGAVA, B., AND YAU, D. 2004. A hybrid architecture for cost-effective on-demand media streaming. *Journal of Computer Networks* 44, 3, 353–382.
- HEFEEDA, M., HABIB, A., BOTEV, B., XU, D., AND BHARGAVA, B. 2003. Promise: Peer-to-peer media streaming using collectcast. In *Proceedings of ACM Multimedia*. 45–54.
- HORNE, B., PINKAS, B., AND SANDER, T. 2001. Escrow services and incentives in peer-to-peer networks. In *Proceedings of ACM Conference on Electronic Commerce (EC)*. 85–94.
- MILOJICIC, D. S., KALOGERAKI, V., LUKOSE, R., NAGARAJA, K., PRUYNE, J., RIHARD, B., ROLLINS, S., AND XU, Z. 2002. Peer-to-Peer Computing. Tech. Rep. HPL-2002-57, HP Labs.
- NGUYEN, T. AND ZAKHOR, A. 2002. Distributed Video Streaming over Internet. In *Proceedings of SPIE/ACM MMCN*. 186–195.
- PADMANABHAN, V. N., WANG, H. J., CHOU, P. A., AND SRIPANIDKULCHAI, K. 2002. Distributing streaming media content using cooperative networking. In *Proceedings of NOSSDAV*. 177–186.
- QIU, D. AND SRIKANT, R. 2004. Modeling and performance analysis of bittorrent-like peer-to-peer networks. In *Proceedings of ACM SIGCOMM*. 367–377.
- RAMACHANDRAN, K. K. AND SIKDAR, B. 2005. An analytical framework for modeling peer-to-peer networks. In *Proceedings of IEEE INFOCOM*.
- RATNASAMY, S., FRANCIS, P., HANDLEY, M., KARP, R., AND SHENKER, S. 2001. A scalable content-addressable network. In *Proceedings of the ACM SIGCOMM*. 161–172.
- RIPEANU, M., FOSTER, I., AND IAMNITCHI, A. 2002. Mapping the gnutella network. *IEEE Internet Computing Journal* 6, 1, 50–57.
- ROWSTRON, A. AND DRUSCHEL, P. 2001a. Pastry: Scalable, decentralized object location and routing for large-scale peer-to-peer systems. In *International Conference on Distributed Systems Platforms (Middleware)*. 329–350.
- ROWSTRON, A. AND DRUSCHEL, P. 2001b. Storage management in past, a large-scale, persistent peer-to-peer storage utility. In *Proceedings of ACM SOSP*. 188–201.
- SAROIU, S., GUMMADI, K. P., AND GRIBBLE, S. D. 2003. Measuring and analyzing the characteristics of napster and gnutella hosts. *Springer/ACM Multimedia Systems* 9, 2 (August), 170–184.
- STOICA, I., MORRIS, R., KARGER, D. R., KAASHOEK, M. F., AND BALAKRISHNAN, H. 2001. Chord: A scalable peer-to-peer lookup service for internet applications. In *Proceedings of the ACM SIGCOMM*. 149–160.
- TRAN, D. A., HUA, K. A., AND DO, T. T. 2003. ZIGZAG: An Efficient Peer-to-Peer Scheme for Media Streaming. In *Proceedings of IEEE INFOCOM*. 1283–1292.
- TU, Y.-C., SUN, J., HEFEEDA, M., AND PRABHAKAR, S. 2005. An analytical study of peer-to-peer media streaming systems. Tech. Rep. CSD-TR-05-011, Department of Computer Sciences, Purdue University.
- TU, Y.-C., SUN, J., AND PRABHAKAR, S. 2004. Performance analysis of a hybrid media streaming system. In *Proceedings of SPIE/ACM MMCN*. 69–82.
- WU, D., HOU, Y. T., ZHU, W., ZHANG, Y.-Q., AND PEHA, J. M. 2001. Streaming Video over the Internet: Approaches and Directions. *IEEE Transactions on Circuits and Systems for Video Technology* 11, 1 (February), 365–386.
- XU, D., CHAI, H.-K., ROSENBERG, C., AND KULKARNI, S. 2003. Analysis of a hybrid architecture for cost-effective streaming media distribution. In *Proceedings of SPIE/ACM MMCN*.
- XU, D., HEFEEDA, M., HAMBRUSCH, S., AND BHARGAVA, B. 2002. On peer-to-peer media streaming. In *Proceedings of IEEE ICDCS*. 363–371.
- YANG, X. AND DE VECIANA, G. 2004. Service capacity of peer to peer networks. In *Proceedings of IEEE INFOCOM*. 2242–2252.